



SYNTHESIS, CHARACTERIZATION AND APPLICATION OF BIMETALLIC OXIDE FOR ADSORPTIVE REMOVAL OF FLUORIDE FROM WATER

***Corresponding Author's :** Abdulkadir Ukule Kedir^{1*}, Kemal Nure Kawo²

^{1*}Department of Chemistry, MaddaWalabu University, Bale Robe, Ethiopia

²Department of Statistics, MaddaWalabu University, Bale Robe, Ethiopia

Email address: abdulkadirukule@gmail.com

Article Received 30-08-2020, Accepted 26-09-2020 , Published 30-09-2020

Abstract

A new bimetallic oxide (calcium aluminate) was synthesized using the combustion method, which offers the formation of smaller particles with open pores. The material thus synthesized and studied for its fluoride uptake properties in spiked and actual drinking waters, containing fluoride ion. The prepared adsorbent material was characterized by Fourier transform infrared (FTIR) Spectroscopy and X-ray diffraction (XRD) Spectroscopy to know the functional group analysis and surface mean crystalline size. A series of batch adsorption experiments were carried out to assess adsorption parameters that influence the adsorption process. The CA shows high adsorption capacity for fluoride ion and it is possible to effectively remove fluoride up to 98% from the initial concentration of 20 mg L⁻¹, using adsorbent dose of 2 g L⁻¹ and 60 min. The experimental data fitted well into Langmuir adsorption isotherm and follows pseudo second order kinetics. The thermodynamic parameters suggest the complex nature of fluoride uptake reaction, dominated by physisorption, spontaneous and endothermic process. The effective regeneration achieved up to 82.5% by treating the fluoride loaded material by NaOH solution. Thus, the most desirable properties of the adsorbent are strong affinity for defluoridation and high adsorption capacity.

Keywords: Adsorption Capacity, Adsorption Isotherm, Bimetallic Oxide, Fluoride removal

1. INTRODUCTION

Fluoride ion (F^-) is one of the most abundant contaminants in water. F^- is a fluorine anion characterized by a small radius, a great tendency to behave as ligand and easiness to form a great number of different organic and inorganic compounds in soil, rocks, air, plants, and animals[1]. Some of those compounds are quite soluble in water, so fluoride is present in surface and groundwater as an almost completely dissociated F^- [1, 2]. In aqueous solution, fluoride is commonly found as fluoride ion. A small amount of fluorine is naturally present in water, air, plants, and animals. As a result, humans are exposed to fluorine through food chains, drinking water and breathing air.

Groundwater plays an important role in the supply of drinking water to rural communities. The use of groundwater is usually regarded as being preferable to the use of surface water in that managed groundwater resources are less vulnerable to contamination and usually require a reduced level of treatment removal of fluorides from water using low-cost adsorbents[3].

Low concentration of F^- in drinking water has been considered beneficial to prevent dental caries [4], but excessive exposure to fluoride can give rise to a number of

adverse effects such as causing fluorosis [5]. Crippling skeletal fluorosis is a significant cause of morbidity in a number of regions of the world. From several studies, it was observed that the average daily dietary intake of fluoride by children residing in fluoridated (1 ppm) communities is $0.05 \text{ mg kg}^{-1}\text{day}^{-1}$; in communities without optimally fluoridated water, average intakes for children were about 50% lower, dietary fluoride intake by adults in fluoridated (1 ppm) areas averages $1.4\text{-}3.4 \text{ mg day}^{-1}$ while in non-fluoridated areas it averages $0.3\text{-}1.0 \text{ mg day}^{-1}$ [6]. WHO has set a limit value of 1.5 mgL^{-1} for fluoride in drinking water [7].

Fluoride concentration above 1.5 mg L^{-1} has been reported from many parts of Ethiopia, but the highest levels are found in the Rift Valley, the low land area with the highest volcanic activity in the country [8]. This region extends from the southwest to the northeast of the countries and dominated by acid volcanic rocks.

The fluoride concentrations of the waters in the Rift Valley, which are supplied from boreholes, were reported to be between 1 and 33 ppm with a mean of 5 ppm [9]. The high fluoride concentration in the Rift system has been attributed to acid volcanic, high temperature rifting, high subsurface carbon dioxide pressure and

low calcium content (due to removal of calcium by carbonate precipitation) and this may suggest that the thermodynamic equilibrium of the fluoride bearing natural rocks are influenced by these factors [10].

Most prevalent de-fluoridation technologies involve Adsorption, Ion exchange, precipitation, Donnan dialysis, Electro dialysis, Reverse osmosis, Nano-filtration and Ultra filtration[11-18]. Adsorption processes are generally more popular because of their efficiency, convenience, simplicity of design and eco-friendly nature. For the adsorbent, the promising ones should have a large adsorption capacity, a wide available pH range, and can be regenerated. Different synthetic adsorbents have been reported for fluoride treatment includes carbon nanotubes, iron oxide, calcium oxide, magnesium oxides, hydrous zirconium oxide, and alumina[19-22]. Mixed metal oxides are being studied because of their potential as advanced materials in fluoride removal. Consequent upon the affinities of calcium (Ca^{2+}) and aluminum (Al^{3+}) for fluoride ion in aqua systems, the performance efficiency of these two metal ions is continually being appraised, as adsorbent, in adsorption based aqua defluoridation processes[23]. The mode of action of this process is hinged on the synergies of lime and alum, which

transformed the aqua fluoride ion into insoluble CaF_2 species and got flocculated. Premised on the hard soft interaction principle (HSIP), developed by Pearson [24], Ca^{2+} and Al^{3+} are classified as hard acid while fluoride ion is a hard base. Thus, the affinity of the metals for the aqua defluoridation could be attributed to the guiding principle regarding the interaction of electron pair donors and acceptors; that the most favorable interactions occur when the acid and base have similar electronic character [25]. Consequently, hard acids preferentially interact with hard bases, and soft acids interact preferentially with soft bases.

In this study; the synthesis, characterization and application of the synthesized bimetallic oxide on its capability for fluoride removal from the water was investigated. Due to the high capability of combined bimetallic oxides to remove fluoride ion from fluoride rich samples, these metal oxides complex with EDTA and Urea as complexing agents were preferred. They were selected due to their: high porosity, large surface area, high degree of surface activity, less toxicity, inertness in nature of aluminum and calcium had the highest affinity toward fluoride ion to form CaF_2 [24]. Thus, calcium containing compound has high capability to adsorb fluoride toward itself

and calcium rich substrates were highest affinity to remove fluoride from fluoride-rich samples. Besides their affinity toward fluoride ion, bimetallic oxide (calcium aluminate) adsorbent was suitable for high adsorption capacity, safe, easy handling, commercially available and environmentally friendly.

2. MATERIALS AND METHODS

2.1 Chemicals and Reagents

All chemicals used in this study were of analytical grade. $\text{AlCl}_3 \cdot 6\text{H}_2\text{O}$ (Banbury Oxon, UK), $\text{CaCl}_2 \cdot 2\text{H}_2\text{O}$ (Alpha chemical India), Ethylene diamine tetra acetic acid and Urea (Alpha chemical India), NaF (Ranchem chemical industry), NaOH (Alphax chemical industry India), $\text{C}_2\text{H}_4\text{O}_2$, NaCl, $\text{Na}_3\text{C}_6\text{H}_5\text{O}_7$ (Alpha chemical India), HCl (Alphax chemical industry India), Palintest Fluoride No. 1 Tablets, Palintest Fluoride No. 2 Tablets.

2.2 Instruments and Apparatus

Filter paper (what man no.42), TLC plate, 10 ml glass tube (PT 595), pH-meter (HANNA instruments HI 83141 UK), Magnetic stirrer (HANNA instruments 300N UK), Drying oven (Digit heat, J. P. Selecta, Spain), Centrifuges, Fluoride ion selective electrode, Palintest Automatic Wavelength Selection Photometer

(Wagtech 7100 England), muffle furnace (CARBOLITE-S33 6RB England), Fourier transformer infrared spectroscopy (Perkin Elmer Spectrum 65 FTIR spectrometer), X-ray diffraction spectroscopy (Philips X-ray diffractometer with $\text{CuK}\alpha$ radiation).

2.3 Synthesis of calcium aluminate

The bimetallic oxide (calcium aluminate) was prepared via the self propagating combustion synthesis method and in-situ hybridization into the framework.

The methodology employed was based on the work of N. Sakhare et al [26] and adapted to this study for adsorbent synthesis. Aqueous solution mixture of 5.91 g calcium chloride dihydrate and 10g aluminum chloride hexahydrate were prepared in 20 mL of deionized water. 3.26 g of Urea and 3.26 g of ethylene diamine tetraacetic acid mixture was also prepared in 20 mL of deionized water and added together to the metal salts solution and mixed thoroughly. The evenly mixed solution was kept in a muffle furnace, at 600 °C for 30 min, for the simultaneous self propagating combustion reaction and the in-situ hybridization of the calcium aluminate framework. The product obtained was ground and homogenized, before transferring it into a muffle furnace for calcination, at 550°C for 3 h. The calcined material was washed with a

copious amount of deionized water and dried at 110°C for 4 h in the drying oven. The material produced was labeled as calcium aluminate and subsequently used as adsorbent in the batch defluoridation process to evaluate its potential as a reactive, permeable material for defluoridation.

2.4 Preparation of fluoride standard solution and Palintest

2.4.1 Preparation of fluoride standard and TISAB solution

A stock solution of fluoride was prepared by dissolving 2.21 g of sodium fluoride in 1 L of deionized water and a working solution of 20 mg L⁻¹ was obtained by appropriate dilution from the stock solution of fluoride. Deionized water was used for all the purposes of this study to avoid any issue related to ionic contamination.

The total ionic strength adjustment buffer (TISAB) was prepared according to a recommended procedure [27] as follows: 57 mL of glacial acetic acid, 58 g of sodium chloride, 7 g of sodium citrate and 2 g of ethylene diamine tetraacetic acid were added to 500 mL of deionized water and allowed to dissolve, and then the pH adjusted to 5.3 with 5 M sodium

hydroxide, and then made up to 1 L in a volumetric flask with deionized water.

2.4.2 Palintest

The procedure employed according to the work of Barghouthi et al [28]. In the Palintest, two tablet reagents were used. The test was simply carried out by adding one of each tablet to a sample of the water. The color produced in the test was indicative of the fluoride concentration and was measured using a Palintest Photometer. The test tube was filled with a sample to the 10 ml mark. Fluoride No. 1 tablet was added, crushed and mixed to dissolve. Fluoride No. 2 tablet was added, crushed and mixed to dissolve. Stand for five minutes to allow full color development. Phot 14 on Photometer was selected and take Photometer reading in the usual manner. The result was displayed as mgL⁻¹ F. To adjust the pH of the solution during the study, 0.1 NaOH and 0.1 HCl were used.

2.5 Analytical methods

The analytical methods employed during and after synthesis, to characterize surface nature of the adsorbent material were Thin layer chromatography (to verify formation of complex), Fluoride ion selective electrode (to check slope), Fourier

transform infrared spectroscopy (for functional group analysis), X-ray diffraction (to calculate mean crystalline size) and Photometer (for determination of residual fluoride) in the spiked water. A pH meter was used to measure the pH of solutions.

2.6 Batch experiments

All batch experiments were conducted in 100 mL Erlenmeyer flask containing 100 mL of fluoride spiked solution at room temperature, to evaluate fluoride removal efficiency and capacity of the adsorbent (calcium aluminate) under continuous mixing condition with magnetic stirrer. The effect of adsorbent dose, initial fluoride concentration, contact time and solution pH were investigated by varying any one of the parameters and keeping the other parameters constant. For each trial, a sample was periodically taken out of the flask and filtered through Whatman no. 42 filter paper for left residual fluoride concentration. All the experiments were performed in triplicates.

The adsorption efficiency (%) and the defluoridation capacity ($\text{mg F}^- \text{ adsorbed g}^{-1}$ of adsorbent) at a given contact time for the selected adsorbents were determined using the following equations [29]:

$$\% \text{ Adsorption} = \frac{C_o - C_t}{C_o} \times 100 \quad [1]$$

$$\text{Defluoridation capacity } \text{mg F}^- \text{g}^{-1} = \frac{C_o - C_t}{m} \quad [2]$$

Where, C_o and C_t are the F^- concentrations initially and at a given time t in mgL^{-1} , respectively and m = dose of adsorbent in gL^{-1} .

2.6.1 Effect of adsorbent dosage

The effect of adsorbent dosage i.e., the amount of the synthesized adsorbent (calcium aluminate) and their active nature on the adsorption of fluoride was studied at different dosages ranging from (0.05, 0.1, 0.15, 0.2, 0.25, 0.3, 0.35 and 0.4) g in 100 mL with initial fluoride concentration of 20 mgL^{-1} solution. After adsorption time was completed the adsorbents were filtered and the concentration of fluoride ion left in solution was determined by Photometer instrument.

2.6.2 Effect of contact time

To examine the effect of contact time, the study was conducted in 100 mL Erlenmeyer flask at (15, 30, 60, 90, 120 and 180 min), with constant adsorbent dosage of ($0.2 \text{ g } 100 \text{ mL}^{-1}$) with initial fluoride concentration of 20 mgL^{-1} solution, temperature $25 \pm 2 \text{ }^\circ\text{C}$. The content

of each flask was filtered and the concentration of residual fluoride ion in each solution was determined by the Photometer instrument.

2.6.3 Effect of pH of the solution

The effect of pH on the adsorption of fluoride onto the solution was studied by varying the initial solution pH range from (3 – 10), by adjusting the pH to the desired level either with 0.1 M NaOH or 0.1 M HCl. For this study 100mL solution with initial fluoride concentrations (20 mgL^{-1}), adsorbent (CA) dose ($0.2 \text{ g}100\text{mL}^{-1}$) and temperature were kept constant at room temperature during the experiment. The residual Fluoride was determined after 1 hr of equilibrium time by the Photometer instrument.

2.6.4 Effect of fluoride initial concentration

Variation of solution concentration was important parameters that affect the quantity of adsorption by the adsorbent material. In this study, fluoride concentrations in the 100mL solution were varied ($2.5, 5, 10, 20 \text{ mgL}^{-1}$) by keeping both contact time and adsorbent dose optimum for 60 min and $0.2 \text{ g}100\text{mL}^{-1}$, respectively. The temperature was kept at room temperature for the experimental conditions and the residual Fluoride ion

concentration was determined after equilibrium time by Photometer instrument.

2.6.5 Effect of Temperature

The effect of variation of solution temperature may affect the adsorption of anions by the materials. Hence to know the variation happen due to temperature difference in the present study, the solution temperature was varied in the temperature of 20, 30 and $40 \text{ }^\circ\text{C}$ in 100mL solution with 0.2 g CA, 60 min equilibrium time and $\text{pH } 7.0 \pm 0.2$. The residual Fluoride ion concentration was determined after equilibrium time by the Photometer instrument.

2.7 Adsorption study

Adsorption isotherm, which shows the relationship between the bulk aqueous phase activity (concentration) of adsorbate and the amount adsorbed at constant temperature. Equilibrium isotherms were studied by taking 100 mL of mixture of fluoride solutions ($2.5, 5, 10, 20, 40, 70$ and 100 mgL^{-1}) in 100 mL Erlenmeyer flasks with $0.2 \text{ g}100\text{mL}^{-1}$ CA, 60 min equilibrium time, $\text{pH } 7.0 \pm 0.2$ and stirred by a magnetic stirrer. The photometer was employed to determine the remaining concentrations of fluoride ions in each sample after adsorption at the desired time

intervals. To establish the adsorption capacity of adsorbents experimental data was fitted against Langmuir and Freundlich isotherm equations and Dubinin Radushkevich (D-R) adsorption isotherm model was used for prediction of removal mechanism.

2.8 Kinetic study

The kinetic study was conducted by taking 100 mL a mixture of fluoride solutions with initial concentrations of (20, 10 and 5) mgL^{-1} in 100 mL Erlenmeyer flasks. Then 0.15, 0.10, 0.05 $\text{g}100\text{mL}^{-1}\text{CA}$, respectively was added to the solution at time intervals of (15, 30, 60, 90, 120 and 180) minutes and the filtrate were analyzed for the remaining fluoride concentrations. The photometer was employed to determine the remaining concentrations of fluoride after adsorption at the desired time intervals. The kinetic analysis of the adsorption data was based on reaction kinetics of pseudo-first-order (not shown) and pseudo-second-order mechanisms. The residual fluoride concentrations were measured as a function of time.

2.9 Thermodynamics study

Thermodynamic study was conducted by taking 100 mL a mixture of fluoride solutions with initial concentrations of 20

mgL^{-1} in 100 mL Erlenmeyerflasks. Then 0.2 g CA was added to the solutions. Solutions were stirred at different temperatures (20, 30, 40 °C) and the filtrate was analyzed for the remaining fluoride concentrations. The photometer was employed to determine the remaining concentrations of fluoride ions in solution after adsorption at the desired time intervals.

2.10 Desorption and readsorption studies

After adsorption, the adsorbate loaded adsorbent was separated from the solution by centrifugation and the supernatant was drained out. The adsorbent was gently washed with distilled water to remove any unabsorbed adsorbate. Regeneration of adsorbate from the adsorbate-loaded adsorbent was carried out using the desorbing media – distilled water at pH 6.95 using 1%, 2% and 3 % solutions of NaOH. Then they were agitated for the equilibrium time of 1Hr and 2Hr. The desorbed adsorbate in the solution was separated and analyzed for the residual fluorides again to study readsorption.

3. RESULTS AND DISCUSSIONS

3.1 Calibration curve

The performance of the electrode was checked initially by calibrating using

standard solutions of fluoride in the range (0.5, 1, 2.5, 5, 10 and 20) mgL^{-1} and to check slope of the adsorbent under study. The electrode potentials of these standard solutions were measured and plotted against the concentration. As can be seen from Figure 1 the electrode performance is good, and the slope of the electrode was 59.83 mV/dec, which is almost closer to the theoretical value (-59.16 mV/dec at 25 °C).

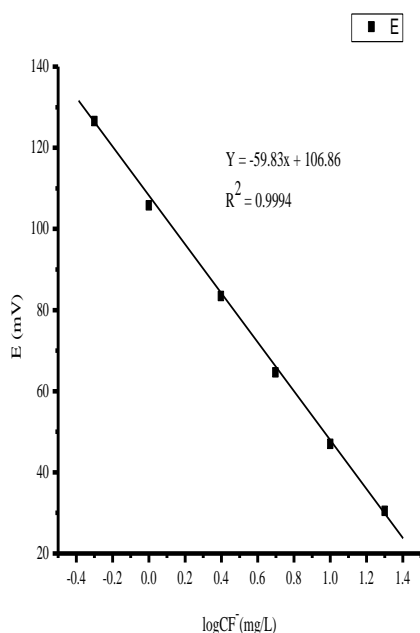


Figure 11 Calibration curves of six standard solutions of fluoride with triplicate measurement.

3.2. Characterization of the Adsorbent

3.2.1 Fourier transform infrared (FTIR) Spectroscopy

The FT-IR spectra of calcium aluminate were measured at 4000-400 cm^{-1} . FT-IR test of CA displays a number of absorption peaks as shown in Figure 2. The result shows that broad peaks at 3420 and 3450 cm^{-1} before and after respectively, exhibit the stretching frequency of -OH and the remaining adsorbed water. The peak observed at $\cong 2500 \text{ cm}^{-1}$ weak sharp was belong to (-C≡N stretching). The peaks observed at 1800 and 1650 cm^{-1} before and after indicates C=O and C=C symmetric stretching respectively.

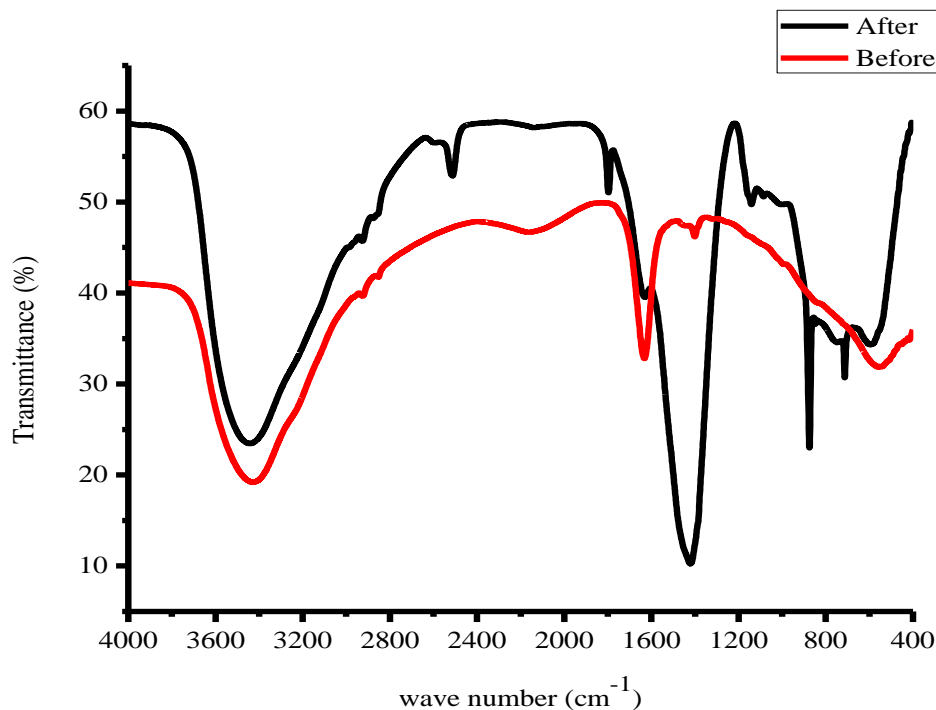


Figure 22 FTIR of CA before and after treatment with fluoride solution

Strong and sharp peak at 1410 cm^{-1} , indicates Antisymmetric and symmetrical vibration of -COO- group was observed. The peaks appear in CA after treatment at 1170 cm^{-1} very short indicates C-F stretching. Peak appear in CA after treatment at 885 cm^{-1} , indicates

O-H out of plane bending. The extra peaks around 700 and 550 cm^{-1} respectively, which indicates the presence of C-Cl and C-F stretching and that was similar with the result of Poursaberi et al [30]. The FT-IR spectra analysis of bimetallic oxide (CA) displays a number of functional groups on their surface indicating the complex nature

of the adsorbent. The adsorption capacity of adsorbent material depends upon porosity as well as the chemical reactivity of functional groups at the CA surface.

3.2.2 X-ray diffraction (XRD) Spectroscopy

The XRD diffractograms were recorded in terms of 2θ in the range $10 - 80$ with a scanning speed of 3.00 deg min^{-1} . The mean crystalline size of the powder was determined by Debye-Scherrer's formula given by equation [3].

$$D = \frac{K\lambda}{\beta \cos\theta} [3]$$

The result below shows a very sharp peak in the reflection angle range for two theta values ($32, 45$, before and around 30 after)

treatment with fluoridated solution, which indicates the high crystallinity order of the synthesized adsorbent. The calculated

mean crystalline size of adsorbent was 62 nm with peak spectra of (211).

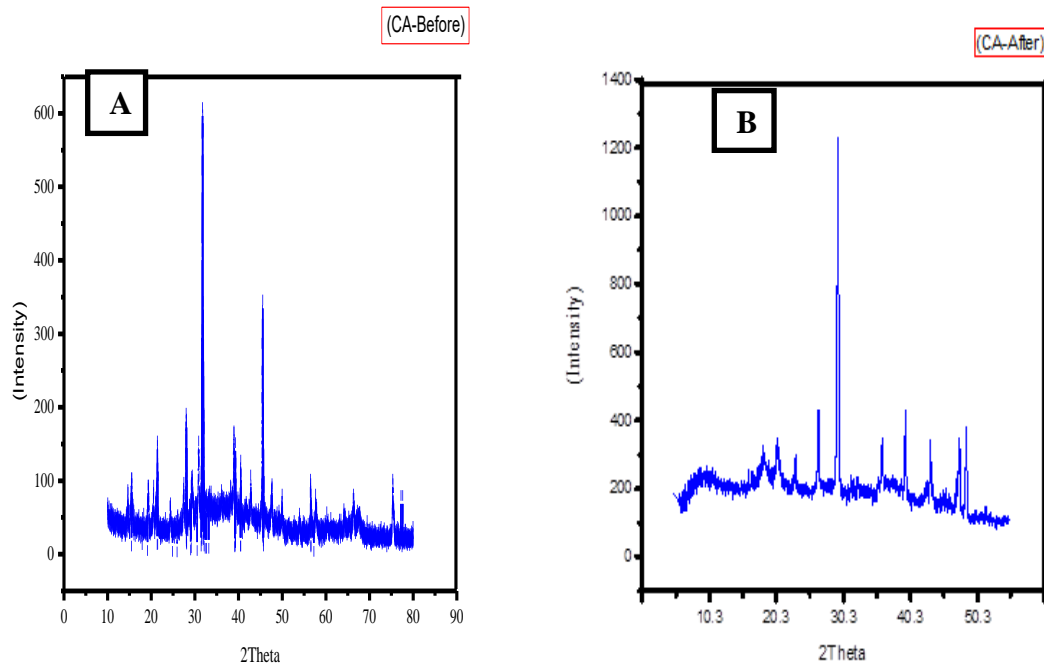


Figure 3 XRD of CA complex (A), before treatment with fluoride (B), after treated with fluoride

the form of calcium and aluminum fluoride salts, which leads to alteration of the crystal structure of CA.

The XRD analysis Fig 3 (A, before treatment and B, after treatment) also reveals that the crystal structure of CA undergoes significant changes after the adsorption of F ions on the surface porous. A sharp peak of F⁻ is seen after absorption, which revealed that F⁻ was absorbed onto adsorbents and was similar to the results of Raghav et al [31]. This infers that the uptake of F ions by CA could be predominantly due to physisorption and in

3.3 Batch adsorption study

3.3.1 Effect of adsorbent dosage

The effect of adsorbent dose on removal of fluoride using bimetallic oxide (calcium aluminate) was shown in Figure 4 below, in which percentage of fluoride removal and capacity (fluoride uptake mg g⁻¹ of adsorbent) were plotted against adsorbent dose. It was observed that percentage removal of fluoride increased with the

increase in adsorbent dose up to 2 g L⁻¹ which was adsorption equilibrium dose, while loading capacity (amount of fluoride loaded per unit weight of adsorbent) gradually decreased for the same way that

may be due to low concentration of fluoride available at higher adsorbent dose and the ability of porous surface almost occupied by the fluoride ion.

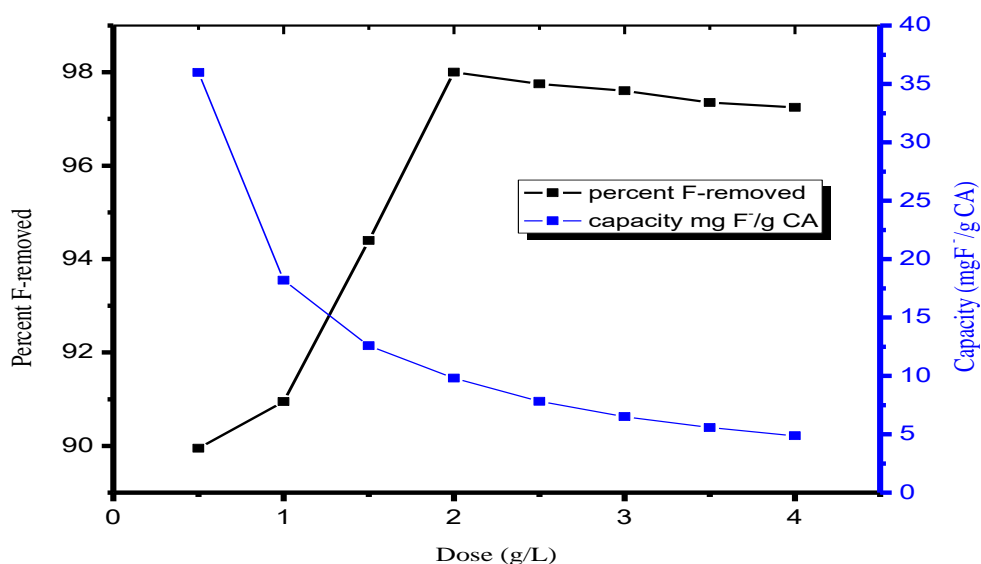


Figure 44 Effect of different doses of CA (Initial fluoride concentration = 20 mg L⁻¹, initial solution pH = 7.0 ± 0.20, Temperature 23 ± 2); all measurement were in triplicate

It was observed that the percentage of fluoride removal increased from 89.95% to 98% with an increase in CA dose from 0.5 to 2 g L⁻¹ at C₀ of 20 mg L⁻¹. This is due to the increase in the active sites to fluoride ion ratio. After optimum dose the graph decrease slightly due to the saturation of surface by fluoride ion. This is consistent with the work of Eva Kumar et al [32] that the increase in fluoride removal efficiency

of the adsorbents with increasing dose might be due to the increase in enhanced active binding sites available for fluoride uptake. The residual 0.4 mg L⁻¹ concentration of fluoride ion remained out of 20 mg L⁻¹ of solution at the optimum dose and equilibrium contact time may also indicate that the calcium aluminate is promising for the removal of fluoride ion from fluoride spiked water to the 1.5 mg L⁻¹ level set by WHO if Ca and Al element is leached to its recommended limits. Hence, 2 g L⁻¹ CA was considered as optimal dose for further studies.

On the other hand, the adsorption capacity decreases with increasing adsorbent dose. To maintain maximum capacity and high removal efficiency the surface loading (i.e. the mass ratio of fluoride to adsorbent dose) should be lower than the optimum value. The surface loading for optimum fluoride removal obtained from Figure 4 is less or equal to 5 mg g⁻¹. A dose of 2 g L⁻¹ corresponding to the capacity of 9.8 mg F⁻ g⁻¹ of the adsorbent were considered for further adsorption studies.

A distribution coefficient K_d, reflects the binding ability of the surface for an element and is dependent on the pH of the solution and type of adsorbent surface. The

distribution coefficient value for fluoride adsorbed on the adsorbent at pH 7 was calculated using the following equation [33]:

$$K_d = \frac{C_s}{C_w} (L/g) \dots \dots \dots [4]$$

Where C_s is the concentration of fluoride on the adsorbent (mg g⁻¹) and C_w is the concentration of fluoride in water (mg L⁻¹). The concentration of fluoride in the solid phase was calculated from the measurement of fluoride in the water before and after the adsorption of fluoride on the adsorbent. Figure 5 shows the value of K_d as a function of adsorbent dose.

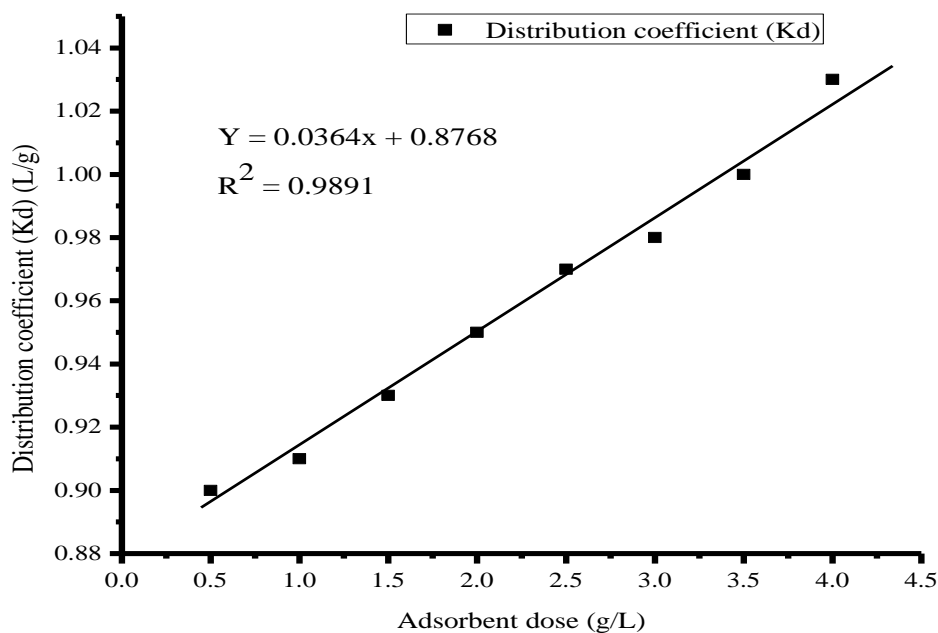


Figure 55 Plot of K_d (Distribution coefficient) value as a function of

adsorbent dose (Initial fluoride concentration = 20 mg L⁻¹, pH = 7.0 ± 0.20)

The result shows that the K_d value increases with an increase in adsorbent dose in the experimental condition indicated at constant pH, which implies the heterogeneous nature of the adsorbent surface. If the surface is homogeneous, the K_d values at a given pH should not change with the adsorbent dose.

3.3.2 Effect of contact time

The effect of contact time on the fluoride removal performance was illustrated in

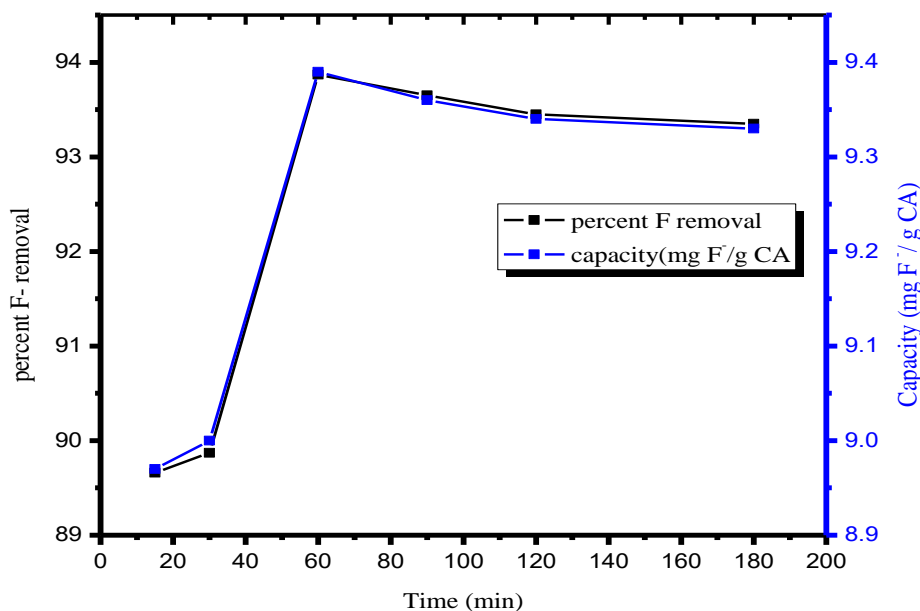


Figure 66 Effect of different contact time (at constant doses of CA 2 g L⁻¹, Initial fluoride concentration = 20 mg L⁻¹, initial

Figure 6. It can be seen that the residual fluoride concentration decreases as contact time increases. The result shows that the uptake of fluoride increased from 89.66% to 93.87% as the contact time between the fluoride and the CA increased from 15 to 180 min. At a time of 60 min, the maximum removal occurred. Beyond 60 min the uptake of fluoride decreased gradually. The high uptake rate at the beginning was attributed due to the high availability of binding sites at the initial stage [34].

solution pH = 7.0 ± 0.20); all measurement were in triplicate.

Thus, as the interaction process progresses the sites for the reaction becomes exhausted resulting in a lower uptake rate of the fluoride after optimum time. After 60 min, further increase in the contact time did not remarkably increase the uptake of fluoride due to the deposition of fluoride ions on the available binding sites of the CA, where it has attained equilibrium. A similar explanation was made by Mahapatra et al[35] for the trend observed on the effect of contact time on the fluoride removal efficiency of the powdered activated charcoal. According to Jamode et al[36] at fixed initial concentration of fluoride and treated bio-adsorbent dose at optimum pH, fluoride removal occurs within the first 60 min which is taken as an equilibrium contact time.

Similarly in the present study, after the sites have been saturated, an equilibrium was established and no further adsorption took place and this may indicate that contact time was one of the factors that affect fluoride removal efficiency of the adsorption. The optimum time for equilibrium concentration was 60 min and it was used in further studies.

3.3.3 Effect of solution pH

The effect of solution pH on the adsorption of fluoride was studied by varying the pH from (3, 4, 5, 6, 7, 8, 9 and 10) by keeping other parameters constant. The results shown in Figure 7 that the strong dependence of removal efficiency on pH was observed within a pH range studied.

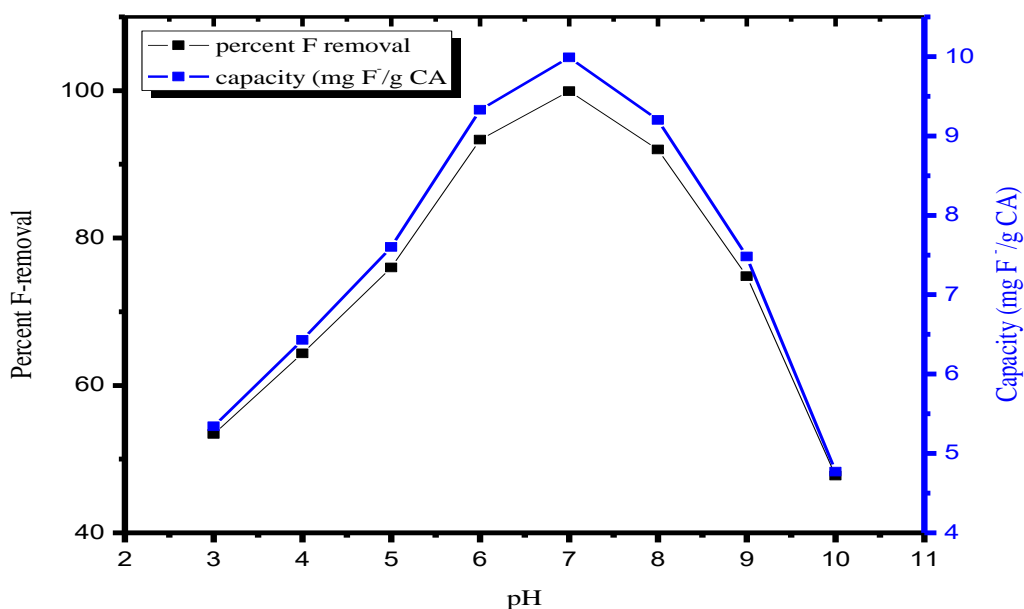


Figure 77 Effect of initial solution pH on fluoride removal efficiency and capacity (dose =2 g L⁻¹, Co = 20 mg L⁻¹, contact time 60 min, shaking speed 150 rpm); all measurement were in triplicate.

The most common single factor that impress the adsorption of ions on the oxide surface was the pH of aqueous solution [37]. The effect of pH on defluoridation was observed that the uptake of fluoride by calcium aluminate was affected below and above neutral. As literature reveals that the pH of the solution significantly affects fluoride uptake capacity [38]. It is evident that the percentage of fluoride removal increase as the pH of the solution increases from 3 to 10 and reaches in maximum at pH 7.0± 0.2. The porous surface of the adsorbent was hindered by the other ions than fluoride at pH varied from neutral. However, it was important to note that the fluoride uptake efficiency at pH 7.0±0.2 was 0.2 mg L⁻¹ which was around 99 % adsorbed. At higher pH (> 7) there was a competition of OH⁻ with F⁻ to occupy the active surface of adsorbent which might not easily remove the expected fluoride ion and at lower pH (< 3), there was formation of HF than binding to the active surface of CA and fluoride ion was not easily removed. The experimental results showed that the fluoride uptake capacity of this study was

more favored within the pH range of 6 to 8, possibly due to the development of positive sites at the surface of the adsorbent. The decrease in the fluoride removal below pH 5 is possibly due to the protonation of the fluoride ion. On the other hand, at a pH above 8, fluoride removal efficiency decreases possibly due to the development of negative charge on the adsorbent surface and/or stronger competition from hydroxide ions. Since both OH⁻ and F⁻ have the same charge and ionic radii [38, 39]. Therefore, the extent of adsorption of fluoride ion on bimetallic oxide (CA) was governed by the pH of the solution near to the neutral pH range.

3.3.4 Effect of initial fluoride solution concentration

The effect of initial fluoride concentrations on the adsorption of fluoride was studied by varying the initial fluoride concentrations (2.5, 5, 10, 20) mg L⁻¹ by keeping other parameters constant. Figure 8 shows the percentage of fluoride removal efficiency and adsorption capacity as a function of initial fluoride concentration at equilibrium. As clearly seen from the Figure 8, there is no significant difference in the percentage of adsorption of fluoride at equilibrium with an increase in initial fluoride concentrations. However, residual concentration at equilibrium increases with

an increase in initial fluoride concentration.

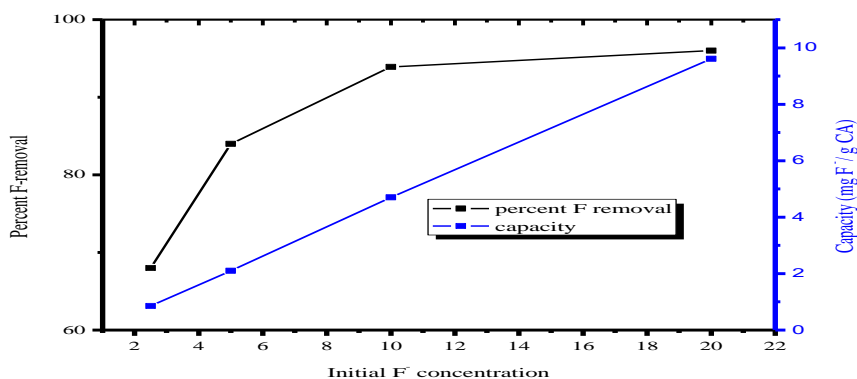


Figure 88 Effect of initial fluoride concentrations at keeping constant (contact time 60 min, adsorbent dose 2 g L⁻¹, temperature 25± 2, pH = 7.0± 0.2 and shaking speed of 150 rpm with a magnetic stirrer); all measurements were in triplicate.

It can be observed that the adsorption capacity has increased with an increase in initial fluoride concentration. This is due to the utilization of less accessible or energetically less active sites because of the increasing diffusivity of fluoride ions when initial concentration increases. The adsorption sites become less difficult to adsorption of the adsorbate upon increasing concentration. This resulted in more fluoride ions to bind per unit mass of the adsorbent (increase in adsorption capacity) when the initial concentration increases. Thus the initial fluoride

concentration had an influence on the equilibrium sorption time, and significant fluoride removal efficiency (96 %) was observed when the initial fluoride is equal to 20 mg L⁻¹ for a contact time of 60 min.

3.4 Adsorption study

Adsorption process is usually studied through graphs known as adsorption isotherm. Adsorption isotherm, which shows the relationship between the bulk aqueous phase activity (concentration) of adsorbate and the amount adsorbed at constant temperature. Adsorption isotherms have many important practical implications; such as they provide information on how the adsorption system proceeds, and indicate how efficiently a given adsorbent interacts with the adsorbate. Adsorption equilibrium provides fundamental physicochemical

data for evaluating the applicability of adsorption processes, usually described by isotherm models whose parameters express the surface properties and affinity of the adsorbent at a fixed operating condition. The model most suitable in a particular case depends on the characteristics of the system. In many cases, the constants contained in the models have direct physical significance. The strength of the linear relationship can be expressed by the correlation coefficient (R^2). Its value is used to evaluate how the isotherm model describes the experimental data.

In this study, Langmuir, Freundlich, and Dubinin-Radushkevich (D-R) adsorption isotherm models were used. The isotherm experiments were carried out at seven different initial fluoride concentrations in a range from (2.5, 5, 10, 20, 40, 70, 100) mg L⁻¹.

3.4.1 Langmuir isotherm

The Langmuir model is based on monolayer adsorption on uniform homogeneous surfaces with sites of identical nature. The Langmuir equation is useful for the estimation of maximum

adsorption capacity corresponding to complete monolayer coverage expressed by:

$$q_e = \frac{q_m b C_e}{1 + b C_e} \quad [5]$$

The linear form of equation (5) gives as:

$$\frac{C_e}{q_e} = \frac{1}{q_m b} + \frac{C_e}{q_m} \quad [6]$$

Where,

C_e is the equilibrium concentration of the adsorbate (mg L⁻¹), q_e is the amount of adsorbate adsorbed per unit mass of adsorbent (mg g⁻¹), q_m and b are Langmuir constants related to adsorption capacity or the amount of a solute adsorbed per unit mass of the adsorbent for monolayer coverage of the surface and heat of adsorption or the binding strength, respectively.

The higher the value of b the higher is the affinity of the adsorbent for the adsorbate. The constants can be determined from the slope and intercept of the C_e/q_e versus C_e plot. The slope of the straight line gives $1/q_m$ and the constant b can be determined from the intercept.

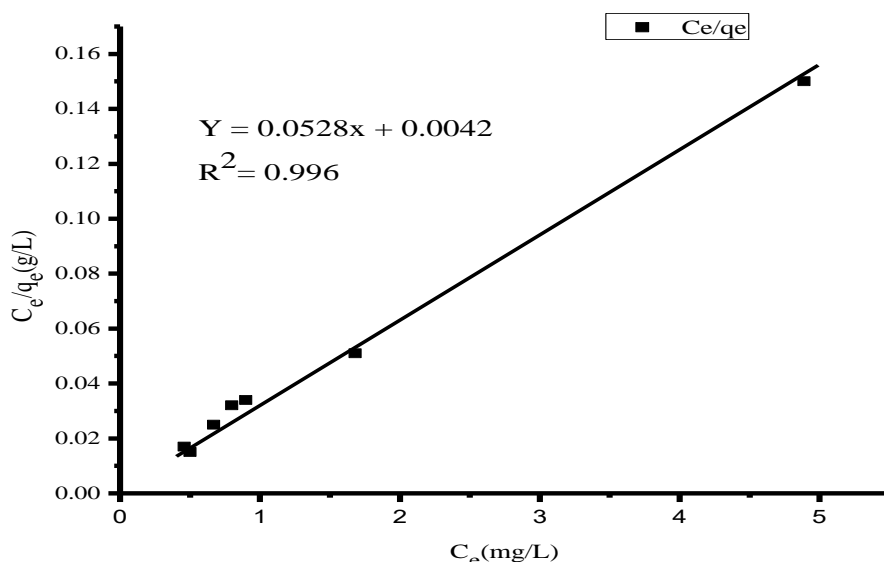


Figure 99 Linear Langmuir isotherm (CA dose = 2 g L⁻¹, contact time 60 min, pH = 7.0 ± 0.20, temperature 23 ± 2, C₀ 20 mg L⁻¹)

Figure 9 shows the Langmuir isotherm model fit for the experimental data. The result of the Langmuir isotherm model shows that the experimental data well fitted to the model with a correlation coefficient (R^2) > 0.99. The maximum sorption capacity corresponding to complete monolayer coverage is found to be 18.93 mg F⁻g⁻¹CA and the constant b related to adsorption intensity is 0.11L mg⁻¹.

Moreover, in order to ensure that the adsorption process is favorable, linear, irreversible or unfavorable for Langmuir kind adsorption process, the essential

characteristics of Langmuir isotherm can be expressed in terms of a dimensionless constant, R_L [40]:

$$R_L = \frac{1}{1 + bC_0} \quad [7]$$

Where C_0 is the initial concentration in mg L⁻¹ and b is the Langmuir constant (L mg⁻¹).

According to Hall et al [40] the parameter R_L indicates the types of the isotherm such that; if $R_L > 1$ it is unfavorable, if $R_L = 1$ it is linear, if $R_L = 0$ irreversible, if $0 < R_L < 1$ it is favorable.

Adsorption of fluoride on the adsorbent under the experimental conditions is favorable, as the value of R_L in all cases is between 0 and 1. Therefore, in this study, the calculated R_L values lie 0.3125 which

is in the range of favorable isotherm condition.

3.4.2 Freundlich Isotherm

The most important multisite or multilayer adsorption isotherm for heterogeneous surfaces is the Freundlich isotherm which is characterized by the heterogeneity factor $1/n$. The basic assumption of this model is that there is an exponential variation in site energies of the adsorbent. The Freundlich equation was presented below in both the standard and linearized form:

$$q_e = k_f C_e^{1/n} \quad [8]$$

Rearranging equation (13) to the linear form of the Freundlich equation:

$$\log(q_e) = \log(k_f) + \frac{1}{n} \log(C_e) \quad [9]$$

Where,

q_e is the amount of fluoride adsorbed per unit mass of adsorbent (mg g^{-1}) at equilibrium, C_e is the equilibrium fluoride concentration (mg L^{-1}), K_F and n are Freundlich constants indicative of adsorption capacity (mg g^{-1}) and adsorption intensity, respectively. When $\log(q_e)$ versus $\log(C_e)$ is plotted a straight line with slope $1/n$ was obtained. Thus, the constants adsorption intensity and adsorption capacity can be determined from the slope and intercept of the graph, respectively. Figure 10 shows the Freundlich isotherm model fit of the experimental data.

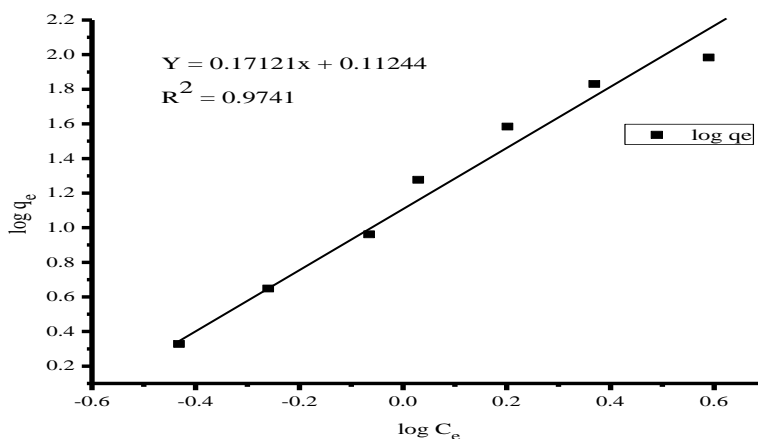


Figure 10 Linear Freundlich isotherm (Adsorbent dose = 2 g L^{-1} , contact time = 60 min, $\text{pH} = 7.0 \pm 0.20$)

The Freundlich parameters along with correlation coefficients were obtained for the adsorbent (Table 1). The result indicated that the experimental fluoride

adsorption data well fitted to this model with the correlation coefficient of 0.9741, suggesting that the average energy of adsorption is decreasing with increasing adsorption density with a minimum adsorption capacity of 9.61 mg g⁻¹ and adsorption intensity, n of 5.841. The value of n obtained lies between 1 and 10 indicating Freundlich favorable sorption. The increase in equilibrium fluoride removal capacity with residual fluoride concentration indicated the heterogeneous nature of the adsorbent surface which is characteristic of adsorption following the Freundlich isotherm model fit as experimental value justify.

3.4.3 Dubinin–Radushkevich (D-R) isotherm

Even if the Freundlich and Langmuir isotherm models are widely used, they do not provide any idea about the adsorption mechanism[41]. Thus, to describe the mechanism of the adsorption process, the equilibrium data was tested with the D-R isotherm model. The D-R model was used to estimate both of the maximum adsorption capacity and the apparent energy of adsorption to distinguish between chemical and physical types of adsorptions[42]. The D-R isotherm assumes, a fixed sorption space close to the sorbent surface is where sorption takes

place. It describes the heterogeneity of sorption energies within this space, which is independent of temperature. The model represented by the equation below:

$$\ln q_e = \ln q_s - \beta \varepsilon^2 \quad [10]$$

Where, q_e and q_s were sorbed concentration and maximum sorption capacity (theoretical saturation) respectively at the sorbent surface, expressed in units of mg g⁻¹ and, β is a constant related to mean free energy of the adsorption, in units of (mol²J⁻²) and ε , is Polanyi potential, is the work required to remove a molecule or ion away from its location in the sorption space. It is calculated as:

$$\varepsilon = RT \ln \left(1 + \frac{1}{C_e} \right) \quad [11]$$

Where R is the universal gas constant (R=8.314 JK⁻¹.mol⁻¹), T is the temperature in Kelvin and C_e is the equilibrium concentration of sorbate in solution.

When $\ln q_e$ is plotted against ε^2 , a straight line may be obtained if the sorption data follow the D-R isotherm. The mean free energy of adsorption per molecule of the sorbate E, is the energy required when the adsorbate migrates to the surface of the adsorbent from infinite distance in the solution to the sorbent surface. Thus it can be correlated and calculated from the β value by using the relation [43]:

$$E = \left(\frac{1}{\sqrt{2\beta}}\right) [12]$$

Figure 11 shows the D-R isotherm plot for the adsorption of fluoride on to CA.

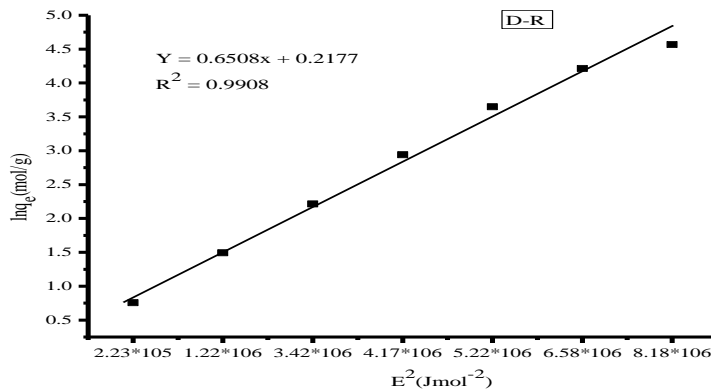


Figure 11 Dubinin-Radushkevich isotherm (CA dose 2g L⁻¹, contact time 60 min, pH 7.0 ± 0.20, T 23± 2°C)

The correlation coefficient, R² value found to be 0.9908, which confirmed that the adsorption process can be described by this model. The sorption capacity evaluated from this model is 96.11 mg g⁻¹. From the magnitude of E, the type of adsorption such as chemical sorption or physical sorption can be determined. If the value of E ranges from (0 - 8 kJmol⁻¹),

sorption is due to physical adsorption and if the value ranges from (9 - 16 kJmol⁻¹), then the adsorption is due to chemical adsorption[44]. The mean free energy of adsorption (E) is found to be 0.87 kJmol⁻¹, which implies that the adsorption is predominantly physisorption.

Table 11 Summary of Freundlich, Langmuir, and D-R isotherm model constants and correlation coefficients for adsorption of fluoride onto CA.

Isotherm model	Constants		Correlation coefficients (R ²)
Langmuir	b (Lmg ⁻¹)	q _m (mgg ⁻¹)	0.9926
	0.11	18.93	
Freundlich	n	K _f (mgg ⁻¹)	0.9741
	5.84	9.61	
Dubinin–Radushkevich (D-R)	q _s (mgg ⁻¹)	E (kJmol ⁻¹)	0.9908
	96.11	0.87	

3.5 Thermodynamic study

Thermodynamic parameters of adsorption, namely standard free energy change (ΔG^0), standard enthalpy change (ΔH^0), and standard entropy change (ΔS^0) were calculated using standard methods. Standard free energy change (ΔG^0) is given by the equation [45]:

$$(\Delta G^0) = -\Delta H^0 + T\Delta S^0 \text{ [13]}$$

The nature of the adsorption of fluoride on the synthesized CA was predicted by estimating the thermodynamic parameters. The changes in thermodynamic parameters such as free energy (ΔG^0), enthalpy (ΔH^0) and entropy (ΔS^0) were evaluated from the following equations:

$$\Delta G^0 = -RT \ln k_c \text{ [14]}$$

Where ΔG^0 standard free energy change of adsorption (kJ mol^{-1}), T is the temperature in Kelvin and R is universal gas constant ($8.314 \text{ Jmol}^{-1}\text{K}^{-1}$) and K_c is the equilibrium constant and calculated as:

$$K_c = \frac{C_{Ae}}{C_e} \text{ [15]}$$

C_{Ae} (mg g^{-1}) and C_e (mg L^{-1}) are the equilibrium concentrations for solute on the adsorbent and in the solution, respectively.

The standard enthalpy change (ΔH), and standard entropy change (ΔS) was calculated using the following equation[45]:

$$\ln k_c = \frac{-\Delta H^0}{RT} + \frac{\Delta S^0}{R} \text{ [16]}$$

The K_c values were used to determine the ΔG^0 , ΔH^0 and ΔS^0 . The K_c expressed in terms of the ΔH^0 (kJmol^{-1}) and ΔS^0 (kJmol^{-1}) as a function of temperature.

ΔH and ΔS were obtained from the slopes and intercepts of the plots of $\ln K_c$ against $1/T$ shown in Figure 12. The free energy change (ΔG) indicates the degree of spontaneity of the adsorption process and the higher negative value reflects a more energetically favorable adsorption. The increase in the negative value of ΔG with an increase of temperature showed that the adsorption of fluoride ion on synthesized CA samples increased with the rise in temperature. The positive values of ΔH shown in Table 2 confirmed the endothermic nature of the adsorbents for fluoride adsorption in the studied range 20 – 40 °C. The positive values of ΔS confirmed the randomness of the adsorption process.

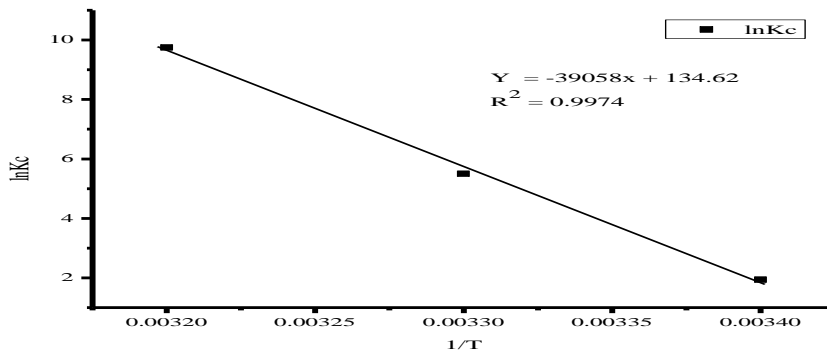


Figure 12 Van't Hoff plot for determination of thermodynamic parameters of equilibrium constant of fluoride ion sorption with temperature (293 - 313 K) (CA dose 2 g L⁻¹, C₀ 20 mg L⁻¹, contact time 60 min, pH 7.0± 0.2).

Table 22 Thermodynamic parameters for sorption of fluoride ion onto CA that are computed from the linearized plot of lnK_c versus 1/T at different temperatures.

ΔG (KJmol ⁻¹)			ΔH (KJmol ⁻¹)			ΔS (Jmol ⁻¹ K ⁻¹)	R ²
293 K	303 K	313K	293 K	303 K	313 K	16.17	0.9994
-1607	-12595	-25372	16.03	15.5	15.01		

3.6 Adsorption kinetics of fluoride

The fluoride adsorption kinetics of adsorbent was studied for each initial fluoride concentrations of 20.0, 10.0 and 5.0 mg L⁻¹ with the corresponding adsorbent dose of (1.5, 1.0 and 0.5) g L⁻¹, respectively. The residual fluoride concentrations as a function of time are shown in Figure 13. The kinetic analysis of the adsorption data is based on reaction kinetics of pseudo-first-order not shown and pseudo-second-order mechanism.

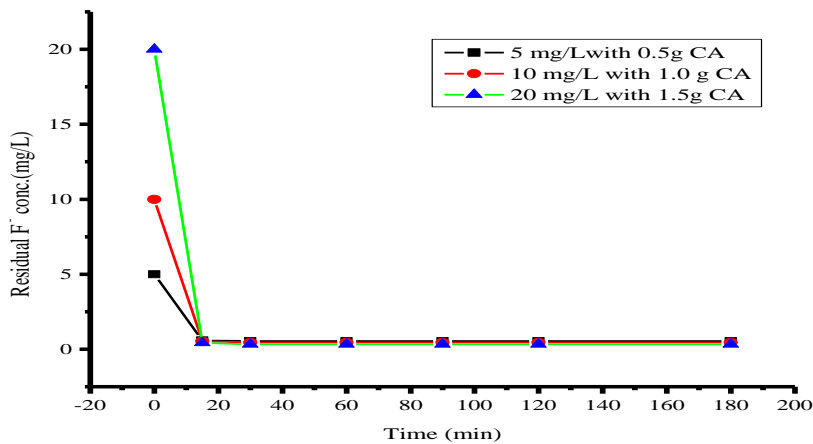


Figure 13 Adsorption kinetics of fluoride on CA adsorbents at constant surface loading 11.08 mg g^{-1} (average pH = 7.0 ± 0.2).

It can be seen in Figure 13 that in all the three cases, initially, the rate of adsorption of fluoride is high during the first 15 minutes. Beyond that, the rate decreases with time, as the liquid phase concentration decreased. From Figure 13, we can also observe that the time to reach equilibrium seems shorter as the concentration becomes lower.

Kinetic analysis of fluoride adsorption was studied based on reaction kinetics of pseudo first order not shown and pseudo second order mechanism using the Lagergren rate equation[46].

3.6.1 Pseudo-first-order

The Lagergren's rate equation is one of the most widely used rate equations to describe the adsorption of adsorbate from the liquid phase [47]. The linear form of pseudo-first-order rate expression of Lagergren is given as:

$$\log(q_e - q_t) = \log(q_e - \frac{k_1 t}{2.303}) [17]$$

Where, q_e and q_t are the amounts of fluoride adsorbed on adsorbent (mg g^{-1}) at equilibrium and at time t (min), respectively, and k_1 is the rate constant of pseudo first-order kinetics which was not shown and the adsorbent fit with pseudo second order.

3.6.2 Pseudo second order

Kinetic analysis of fluoride adsorption was studied based on reaction kinetics of

pseudo-second-order mechanism using the Lagergren rate equation as shown below.

$$\frac{d(q_e - q_t)}{dt} = k_2(q_e - q_t)^2 \quad [18]$$

$$\frac{d(q_e - q_t)}{(q_e - q_t)^2} = -k_2 dt \quad [19]$$

The integrated form at boundary conditions ($t = 0$ to $t = t$ and $q_t = 0$ to $q_t = q_t$) gives:

$$\frac{1}{(q_e - q_t)} = \frac{1}{q_e} + k_2 t \quad [20]$$

$$\frac{t}{q_t} = \frac{1}{k_2 q_e^2} + \frac{t}{q_e} \quad [21]$$

Where, q_e and q_t are the amount of adsorbed fluoride at equilibrium and any time t (mg g^{-1}), respectively, k_2 is the rate constant ($\text{g mg}^{-1} \text{min}^{-1}$), t is the stirring time (min). K_2 can be determined by plotting t/q_t against t based on equation [26]. The larger the k_2 value, the slower the adsorption rate.

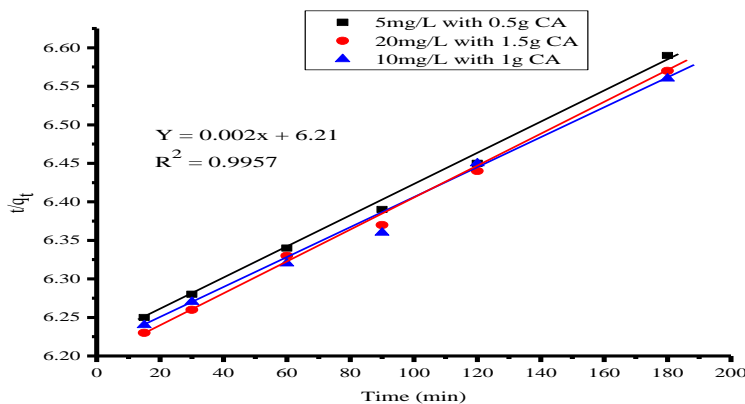


Figure 1414 Pseudo second order plot of fluoride adsorption kinetics on the adsorbent each with initial fluoride concentrations of (5, 10 and 20) mg L^{-1} , to adsorbent doses of (0.5, 1 and 1.5) g L^{-1} , respectively ($\text{pH} = 7.0 \pm 0.20$, contact time = 60 min)

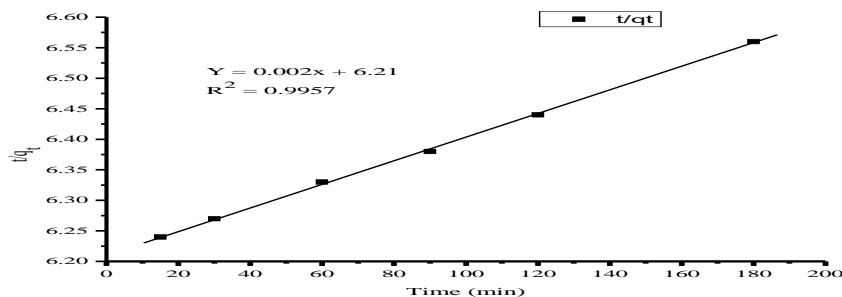


Figure 15 Average pseudo second order plot of fluoride adsorption kinetics on adsorbents (pH = 7.0 ± 0.2, contact time = 60 min).

Table 33 Pseudo-second order rate constants, rate equations, correlation coefficients and their averages for the three different initial fluoride concentrations.

Adsorbate(mgL ⁻¹) / adsorbent(gL ⁻¹)	Rate constant (k ₂)(g mg ⁻¹ min ⁻¹)	Rate equation	Correlation coefficients (R ²)
5/ 0.5	5.15x10 ⁻⁴	t/q _t = 0.002t+ 6.198	0.9967
10 /1.0	8.81x10 ⁻⁵	t/q _t = 0.0019t + 6.2213	0.9994
20 / 1.5	2.71x10 ⁻⁵	t/q _t = 0.00198t + 6.2059	0.9912
Average	2.1x10 ⁻⁴	t/q _t = 0.002t + 6.21	0.9957

3.7 Desorption studies

Regeneration of adsorbate from the adsorbate-loaded adsorbent was carried out using the desorbing media distilled water at pH 6.95 using 1%, 2% and 3% solutions of NaOH with duration of 1Hr and 2Hr. The results of the desorption of fluoride under various concentrations of NaOH and different conditioning durations are indicated in the Figure 16.

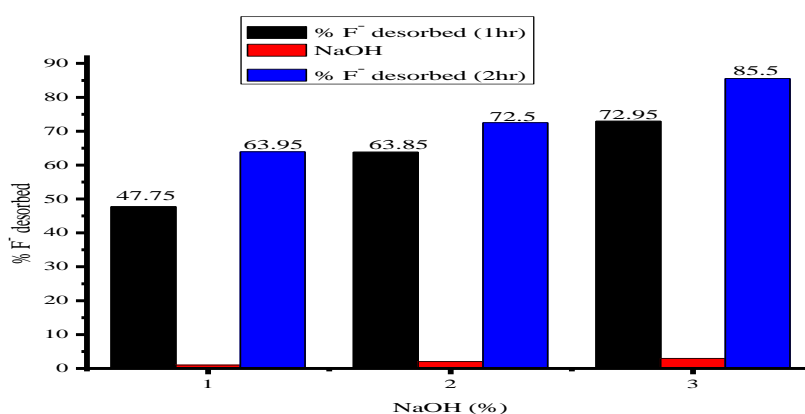


Figure 16 Percentage of fluoride desorbed with different concentrations of NaOH solution after 1 Hr and 2Hr

It can be seen from Figure 16 that desorption was highest at 3% NaOH after 2Hr. The displacement of adsorbed fluoride from the solid surface seems a slower process as compared to adsorption.

About 85.55% of fluoride was desorbed from the adsorbent after 2Hr. Although the result indicates that the possibility of increased desorption as the contact time increases, further studies on multicycles use will be required to optimize the desorption process for the efficient utilization of the adsorbent.

The regenerated adsorbent was investigated for its readsorption capacity to assess its reuse potential. It was found that the adsorption efficiency is 82.45% during the second cycle, which suggests that the adsorbent can be capability for reused. From the results of desorption and readsorption, it can be concluded that regeneration and reuse were promising for the adsorbent under study.

3.8 Comparison of CA defluoridation capacities with the other reported adsorbents

The fluoride ion adsorption capacity of different adsorbent varies according to the nature of the sorbent since it depends on the affinity of each adsorbent to fluoride ions. Thus comparison of the defluoridation capacity of different sorbents is fundamental to evaluate their relative potential and for the selection of adsorbents as a defluoridating agent. Hence the adsorption capacity of few sorbents was compared, which are investigated by different studies. The optimum contact time required for the adsorption of fluoride (equilibrium time) was also compared as indicated in Table 4.

Table 44 Comparison of adsorption capacities of a few adsorbents with different calcium and aluminum rich adsorbents in aqua defluoridation.

Adsorbents	Adsorption capacity(mg g ⁻¹)	Equilibrium time (Hr)	Reference
Natural(analcite and Mordenite) zeolite	0.47	20	[48]
Hydrated alumina	23.75	1	[38, 49]
Activated Alumina(OA-25)	1.45	6	[49]

AILS	84.03	10	[38]
Al modified Bone char	0.97	72	[50]
Bimetallic oxide (CA)	4.48	1	present study

The adsorptive capacity of bimetallic CA to remove fluoride has been compared with those of other adsorbents reported in the literature (Table 4) based on the Langmuir isotherm models. It can be seen that bimetallic oxide exhibits considerably greater F^- adsorption potential as compared to other adsorbents except locally hydrated alumina and aluminum hydroxide impregnated limestone. It was important to emphasize that the particle size, surface area, surface properties, coordination, etc., get modified when material dimensions reach nano size by calcination at a higher temperature scale. Thus compared with the traditional micro sized materials used for sorption processes, nano sized carriers possess a good performance due to high surface area to volume ratio and absence of internal diffusion resistance [32].

4. CONCLUSIONS AND RECOMMENDATIONS

4.1 Conclusions

The new bimetallic oxide (CA) type adsorbent was synthesized by using the combustion method and the method has resulted in fine oxide like structure and highly porous material, which is important

for efficient mass transfer. Characterization results show that the ISE experiment indicated that the slope - 59.83mV/dec which was in the Nernst slope range, X-ray diffraction and FTIR characterization studies infer that the formation of some amount of new species after treatment with fluoride spiked sample, which further suggests the nature of fluoride uptake by the adsorbent. The CA shows high uptake of fluoride and it was possible to remove fluoride ion up to 98% of fluoride from the initial concentration of 20mg L⁻¹ and optimum dose of 2 g L⁻¹, 60 min.

The adsorption isotherm fitted well to Langmuir isotherm model from correlation coefficient output. The Dubinin Radushkevich isotherm model also provides fluoride removal mechanism and the adsorption process has adsorption energy value 0.87 kJmol⁻¹ for fluoride ion, indicating the adsorption process is predominantly physisorption which the adsorbent takes place through surface adsorptions.

The kinetic studies showed that the adsorption of fluoride on the adsorbent was well described by the pseudo-second-order reaction mechanism. The thermodynamic studies revealed from the value of ΔH , ΔS , and ΔG that adsorption of fluoride ion by CA were endothermic and spontaneous process. Desorption was taken place by different percent of NaOH solution and regeneration of CA was also possible and up to 82.45 % regeneration could be achieved. So it can be concluded that CA would be an alternative adsorbent of defluoridation from fluoride-rich water.

4.2 Recommendations

Most peoples in the rift valley regions of the country are victims of the health impact imposed on them from excess fluoride in their drinking water. Most of rural peoples in the rift valley region use groundwater as drinking without any defluoridation treatment. Thus, bimetallic oxide as adsorbent material was used as one of the defluoridation mechanism. Contributing to a sustainable solution for fluoride problem in the area by some responsible and concerned organizations, institutions, and individuals were encouraged and they have to strengthen their role to mitigate the problem in the area. Regarding the adsorbent studied, further studies on; the stability of the adsorbent, use of calcium

aluminate in a column operational mode at the lab scale and scaling up, assessing the amount of calcium and aluminum metal unleached that may be above or below the permissible limit for consumption.

REFERENCES

1. International Programme on Chemical, S., Fluorides. 2002, World Health Organization: Geneva.
2. International Programme on Chemical, S., et al., Fluorine and fluorides / published under the joint sponsorship of the United Nations Environment Programme, the International Labour Organisation, and the World Health Organization. 1984, World Health Organization: Geneva.
3. Nemade, P., Removal of fluorides from water using low cost adsorbents, in Water Science & Technology Water Supply. 2002. p. 311-317.
4. Bellack, E. and P.J. Schouboe, Rapid Photometric Determination of Fluoride in Water. Use of Sodium 2-(p-Sulfophenylazo)-1,8-dihydroxynaphthalene-3,6-disulfonate-Zirconium Lake. Analytical Chemistry, 1958. **30**(12): p. 2032-2034.

5. Agarwal, M., et al., Defluoridation of Water Using Amended Clay. *Journal of Cleaner Production*, 2003. **11**: p. 439-444.
6. Dean, J.A., J. Jones, and L. Walker Vinson, McDonald and Avery's Dentistry for the Child and Adolescent: Tenth Edition. 2015. 1-700.
7. Larsen, M.J., Defluoridation of water at high pH with use of brushite, calcium hydroxide, and bone char. *J.Dent.Res.*, 1993. **72**: p. 1519-1525.
8. Reimann, C., et al., Drinking water quality in the Ethiopian section of the East African Rift Valley I— data and health aspects. *Science of The Total Environment*, 2003. **311**(1): p. 65-80.
9. Gizaw, B., The origin of high bicarbonate and fluoride concentrations in waters of the Main Ethiopian Rift Valley, East African Rift system. *Journal of African Earth Sciences*, 1996. **22**(4): p. 391-402.
10. Selinus, O., Medical Geology: An Opportunity for the Future. *AMBIO: A Journal of the Human Environment*, 2007. **36**(1): p. 114-116, 3.
11. Meenakshi, S. and N. Viswanathan, Identification of selective ion-exchange resin for fluoride sorption. *Journal of Colloid and Interface Science*, 2007. **308**(2): p. 438-450.
12. Sujana, M.G., R.S. Thakur, and S.B. Rao, Removal of Fluoride from Aqueous Solution by Using Alum Sludge. *Journal of Colloid and Interface Science*, 1998. **206**(1): p. 94-101.
13. Durmaz, F., et al., Fluoride removal by donnan dialysis with anion exchange membranes. *Desalination*, 2005. **177**(1): p. 51-57.
14. Zeni, M., et al., Study on fluoride reduction in artesian well—water from electro dialysis process. *Desalination*, 2005. **185**(1): p. 241-244.
15. Simons, R., Trace element removal from ash dam waters by nanofiltration and diffusion dialysis. *Desalination*, 1993. **89**(3): p. 325-341.
16. Guo, Y., et al., Adsorption of Cr(VI) on micro- and mesoporous rice husk-based active carbon. *Materials Chemistry and Physics*, 2003. **78**(1): p. 132-137.
17. Oladoja, N.A. and A.L. Ahmad, Gastropod shell as a precursor for the synthesis of binary alkali-earth and transition metal oxide for

- Cr(VI) Abstraction from Aqua System. Separation and Purification Technology, 2013. **116**: p. 230-239.
18. Steenbergen, F., R. Tekle-Haimanot, and A. Sidelil, High Fluoride, Modest Fluorosis: Investigation in Drinking Water Supply in Halaba (SNNPR, Ethiopia). Journal of Water Resource and Protection, 2011. **3**: p. 120-126.
 19. Li, Y.-H., et al., Adsorption of fluoride from water by aligned carbon nanotubes. Materials Research Bulletin, 2003. **38**(3): p. 469-476.
 20. Patel, G., U. Pal, and S. Menon, Removal of Fluoride from Aqueous Solution by CaO Nanoparticles. Separation Science and Technology, 2009. **44**(12): p. 2806-2826.
 21. Dou, X., et al., Remediating fluoride from water using hydrous zirconium oxide. Chemical Engineering Journal, 2012. **198-199**: p. 236-245.
 22. Jagtap, S., et al., Fluoride in Drinking Water and Defluoridation of Water. Chemical Reviews, 2012. **112**(4): p. 2454-2466.
 23. Turner, B.D., P. Binning, and S.L.S. Stipp, Fluoride Removal by Calcite: Evidence for Fluorite Precipitation and Surface Adsorption. Environmental Science & Technology, 2005. **39**(24): p. 9561-9568.
 24. Pearson, R.G., Hard and soft acids and bases, HSAB, part 1: Fundamental principles. Journal of Chemical Education, 1968. **45**(9): p. 581.
 25. Cahill, C.L., Descriptive Inorganic Chemistry (James E. House and Kathleen A. House). Journal of Chemical Education, 2004. **81**(5): p. 647.
 26. Sakhare, N., et al., Defluoridation of water using calcium aluminate material. Chemical Engineering Journal, 2012. **203**: p. 406-414.
 27. Gude, V.G. and N. Nirmalakhandan, Desalination at low temperatures and low pressures. Desalination, 2009. **244**(1): p. 239-247.
 28. Barghouthi, Z. and S. Amereih, Field method for estimation of fluoride in drinking groundwater by photometric measurement of spot on aluminium quinalizarin reagent paper. Arabian Journal of Chemistry, 2017. **10**: p. S2919-S2925.
 29. Fan, X., D.J. Parker, and M.D. Smith, Adsorption kinetics of

- fluoride on low cost materials. *Water Research*, 2003. **37**(20): p. 4929-4937.
30. Poursaberi, T., et al., Development of zirconium (IV)-metalloporphyrin grafted Fe₃O₄ nanoparticles for efficient fluoride removal. *Chemical Engineering Journal*, 2012. s **189–190**: p. 117–125.
 31. Raghav, S. and D. Kumar, Comparative kinetics and thermodynamic studies of fluoride adsorption by two novel synthesized biopolymer composites. *Carbohydrate Polymers*, 2019. **203**: p. 430-440.
 32. Kumar, E., et al., Defluoridation from aqueous solutions by nano-alumina: Characterization and sorption studies. *Journal of Hazardous Materials*, 2011. **186**(2): p. 1042-1049.
 33. Stumm, W., Reactivity at the mineral-water interface: dissolution and inhibition. *Colloids and Surfaces A: Physicochemical and Engineering Aspects*, 1997. **120**(1): p. 143-166.
 34. Yadav, A.K., et al., Removal of fluoride from aqueous solution and groundwater by wheat straw, sawdust and activated bagasse carbon of sugarcane. *Ecological Engineering*, 2013. **52**: p. 211-218.
 35. Mahapatra, A., B.G. Mishra, and G. Hota, Studies on Electrospun Alumina Nanofibers for the Removal of Chromium(VI) and Fluoride Toxic Ions from an Aqueous System. *Industrial & Engineering Chemistry Research*, 2013. **52**(4): p. 1554-1561.
 36. Tiwari, K.K., et al., Defluoridation of water using inexpensive natural material. *Electronic Journal of Environmental, Agricultural and Food Chemistry*, 2011. **10**(11): p. 3104-3112.
 37. Çengelöğlü, Y., E. Kır, and M. Ersöz, Removal of fluoride from aqueous solution by using red mud. *Separation and Purification Technology*, 2002. **28**(1): p. 81-86.
 38. Jain, S. and R.V. Jayaram, Removal of Fluoride from Contaminated Drinking Water using Unmodified and Aluminium Hydroxide Impregnated Blue Lime Stone Waste. *Separation Science and Technology*, 2009. **44**(6): p. 1436-1451.
 39. Meenakshi and R.C. Maheshwari, Fluoride in drinking water and its removal. *Journal of Hazardous Materials*, 2006. **137**(1): p. 456-463.

40. Hall, K.R., et al., Pore- and Solid-Diffusion Kinetics in Fixed-Bed Adsorption under Constant-Pattern Conditions. *Industrial & Engineering Chemistry Fundamentals*, 1966. **5**(2): p. 212-223.
41. Bharat, T.V., Selection and Configuration of Sorption Isotherm Models in Soils Using Artificial Bees Guided by the Particle Swarm. *Adv. in Artif. Intell.*, 2017. **2017**: p. 1.
42. Chen, S.G. and R.T. Yang, Theoretical Basis for the Potential Theory Adsorption Isotherms. The Dubinin-Radushkevich and Dubinin-Astakhov Equations. *Langmuir*, 1994. **10**(11): p. 4244-4249.
43. Hobson, J.P., Physical adsorption isotherms extending from ultrahigh vacuum to vapor pressure. *The Journal of Physical Chemistry*, 1969. **73**(8): p. 2720-2727.
44. Tripathy, S.S. and A.M. Raichur, Abatement of fluoride from water using manganese dioxide-coated activated alumina. *Journal of Hazardous Materials*, 2008. **153**(3): p. 1043-1051.
45. Yang, M., et al., Fluoride removal in a fixed bed packed with granular calcite. *Water Research*, 1999. **33**(16): p. 3395-3402.
46. Mohapatra, D., et al., Use of oxide minerals to abate fluoride from water. *Journal of Colloid and Interface Science*, 2004. **275**(2): p. 355-359.
47. Lagergren, S.K., About the Theory of So-called Adsorption of Soluble Substances. *Sven. Vetenskapsakad. Handlingar*, 1898. **24**: p. 1-39.
48. Gómez-Hortigüela, L., et al., Natural zeolites from Ethiopia for elimination of fluoride from drinking water. *Separation and Purification Technology*, 2013. **120**: p. 224-229.
49. Ghorai, S. and K.K. Pant, Investigations on the column performance of fluoride adsorption by activated alumina in a fixed-bed. *Chemical Engineering Journal*, 2004. **98**(1): p. 165-173.
50. López Valdivieso, A., et al., Temperature effect on the zeta potential and fluoride adsorption at the α -Al₂O₃/aqueous solution interface. *Journal of Colloid and Interface Science*, 2006. **298**(1): p. 1-5.